Carbon balance of a grazed savanna grassland ecosystem in South Africa

Matti Räsänen[1], Mika Aurela[2], Ville Vakkari[2], Johan P. Beukes[3], Juha-Pekka Tuovinen[2], Pieter G. Van Zyl[3], Miroslav Josipovic[3], Andrew D. Venter[3], Kerneels Jaars[3], Stefan J. Siebert[3], Tuomas Laurila[2], Janne Rinne[1,2,4,5], and Lauri Laakso[2,3]

[1]Department of Physics, University of Helsinki, Finland
[2]Finnish Meteorological Institute, Helsinki, Finland
[3]Unit for Environmental Sciences and Management, North-West University, South Africa
[4]Department of Geosciences and Geography, University of Helsinki, Finland
[5]Department of Physical Geography and Ecosystem Science, Lund University, Sweden

Correspondence to: Matti Räsänen (matti.rasanen@helsinki.fi)

Abstract. Tropical savannas and grasslands are estimated to contribute significantly to the total primary production of all terrestrial vegetation. Large parts of African savannas and grasslands are used for agriculture and cattle grazing, but the carbon flux data available from these areas is limited. This study explores carbon dioxide fluxes measured with the eddy covariance method for three years at a grazed savanna grassland in Welgegund, South Africa. The tree cover around the measurement site, grazed by cattle and sheep, was around 15 %. The night-time respiration was not significantly dependent on either soil moisture or soil temperature on a weekly temporal scale, whereas on an annual time scale higher respiration rates were observed when soil temperatures were higher. The carbon dioxide balances of the years 2010–11, 2011–12 and 2012–13 were -85 ± 16, 67 ± 20 and 139 ± 13 g C m^{-2} yr^{-1}, respectively. The yearly variation was largely determined by the changes in the early wet season fluxes (September to November) and in the mid-growing season fluxes (December to January). Early rainfall enhanced the respiratory capacity of the ecosystem throughout the year, whereas during the mid-growing season high rainfall resulted in high carbon uptake.

1 Introduction

Savannas are highly dynamic ecosystems which cover about 40 % of Africa and 20 % of the global land area (Scholes and Walker, 1993). The savanna ecosystems are generally characterized by alternating wet and dry seasons, during the latter of which wildfires can occur. There can also be transitional seasons between the wet and dry seasons. There are large differences between savannas in terms of their tree cover, species composition and soil type. Furthermore, large parts of African savannas have been inhabited by humans throughout the evolution of our species and thus are modified by activities such as grazing and logging.

Overall, the African continent is estimated to be a small sink of atmospheric carbon, although the uncertainty of this estimate is high due to the lack of long-term measurements in many key ecosystems of the continent (Valentini et al., 2014). The tropical savannas and grasslands are estimated to account for 30 % of the global primary production of all terrestrial vegetation (Grace et al., 2006). In addition, it has recently been shown that the inter-annual variability of the terrestrial carbon cycle is dominated by semi-arid ecosystems (Ahlström, 2015).

The main meteorological drivers of the carbon fluxes between the atmosphere and African savannas are precipitation, soil moisture and soil temperature (Merbold et al., 2009). The maximum carbon assimilation rates in a range of different African ecosystems have been shown to be an exponential function of the mean annual rainfall (Merbold et al., 2009). While the total ecosystem respiration was observed to be exponentially dependent on the soil temperature at seasonal time scales in South African savanna (Kutsch et al., 2008). Archibald et al. (2009) did not consider the conventional exponential function an appropriate representation of the temperature response. Instead, they found that a generalized Poisson function was a better descriptor of the effect of temperature on respiration, as it describes both the exponential increase of respiration with the temperature and its decrease at higher temperatures.

Net Ecosystem Exchange (NEE) has been determined by eddy covariance at various savanna sites (Ago et al., 2014; Archibald et al., 2009; Brümmer et al., 2008; Quansah et al., 2015; Tagesson et al., 2015; Tagesson et al., 2016; Veenendaal et al., 2004). Many of the Sahelian measurement sites are affected by grazing or agriculture, whereas all the Southern African sites are located inside national parks or nature reserves. However, large parts of Southern African savannas are used for agriculture and grazing; for example in South Africa 80 % of the land surface is taken up by farmlands (Kotze and Rose, 2015).

The yearly sum of NEE has been observed to range between -429 (sink) and +155 (source) g C m^{-2} yr^{-1} across eight sites in semi-arid African savannas (Archibald et al., 2009; Brümmer et al., 2008). Archibald et al. (2009) found that the main drivers of inter-annual variation in NEE are the amount of absorbed Photosynthetically Active Radiation (PAR), length of the growing season and the number of days in the year when moisture was available in the soil. Tagesson et al. (2016) synthesized data from six different sites across the Sahel and found the yearly NEE sum to range between -373 and -10 g C m^{-2} yr^{-1}. The variability of NEE was strongly linked to changes in Gross Primary Production (GPP) which was regulated by

vegetation phenology and soil moisture dynamics. However, the environmental drivers for the inter-annual variation in NEE are poorly understood.

To understand these human-influenced savanna ecosystems, we analysed three years of eddy covariance CO_2 flux data from a grazed semi-arid savanna in central southern Africa. The carbon balance of this ecosystem was determined for three yearly periods and its response to the environmental drivers was analysed at diurnal, monthly and inter-annual time scales. The longer-term productivity at the measurement site was assessed using a remotely sensed Normalised Differential Vegetation Index (NDVI) as proxy for GPP. The main objective of this study is to quantify the carbon balance and its inter-annual variation in a grazed semi-arid savanna ecosystem and to find possible climatic drivers for this variation.

2 Materials and methods

2.1 Site description

The Welgegund atmospheric measurement station (26°34'10"S, 26°56'21"E, 1480 m a.s.l.; www.welgegund.org) in South Africa has been measuring atmospheric aerosols and trace gases since May 2010. This site is located on a flat savanna grassland plain which is grazed by cattle and sheep. The monthly mean temperature and precipitation at a nearby weather station during 1998–2014 are shown in Fig. 1. In general, the rainy season lasts from October to April, coinciding with the highest temperatures, but there can be substantial amount of rain as early as in September. This is followed by the dry and cooler season from May to September. The mean annual rainfall was 540 mm with a standard deviation of 112 mm between 1998 and 2014. During this period, on average, 93 % of the yearly rainfall occurred between October and April. The main wind direction was from the north-west during daytime and the north-east during night-time. The aerodynamic roughness length was estimated to be 0.42 m assuming no zero-plane displacement height.

The measurement site is located at a commercial farm which has about 1300 head of cattle which varies ± 300 depending on the year. During a wet year there are more animals than during a dry year. The cattle are grazing on an area of approximately 6000 ha, which consists of natural grazing (e.g. at the measurement site), planted grazing and maize/sunflower fields that are grazed after harvesting. This form of farming is considered large-scale commercial farming. Due to the semi-arid climate, the carrying capacity of the grazing fields tends to be low and thus the grazing area is large. The farmers cannot keep track of the grazing patterns, but they do move the cattle around to optimize grazing and protect the field against overgrazing.

The area around the eddy covariance measurement tower is dominated by perennial C_4 grass species (Table 1). The dominant grass species are *Eragrostis trichophora*, *Panicum maximum* and *Setaria sphacelata.* There is also a considerable amount of forbs, of which the dominant species are *Dicoma tomentosa*, *Hermannia depressa*, *Pentzia globosa* and *Walafrida densiflora*. This grassland type is referred to as a thornveld. It has a tree cover above 15 % and an average tree height of 2.5 m. The common tree species are *Vachellia erioloba*, *Searsia pyroides* and *Celtis africana*.

The soil organic carbon content was 0.93 % and the pH was 5.69. Detailed descriptions of the soil texture and chemical composition around the measurement site are given in Table S1. The soil around the site is loamy sand.

Based on the vegetation sampling described in Sect. S1, the LAI within the flux footprint had a maximum value of 2.32 m^2 m^{-2} in April and a minimum of 0.37 m^2 m^{-2} in July (Table 2). The leaf biomass followed the same trend, with a maximum value of 644 g m^{-2} and a minimum of 233 g m^{-2} (Table 2).

2.2 Instrumentation

At the measurement site there are continuous measurements of atmospheric aerosols, trace gases and meteorology (Booyens et al., 2015; Jaars et al., 2014; Laakso et al., 2013; Vakkari et al., 2014, 2015). In this paper, we present the data directly relevant to carbon cycle dynamics from September 2010 to August 2013.

The meteorological measurements included air temperature (Rotronic MP 101A) and pressure (Vaisala PTB100B), wind speed (Vector A101ML) and direction (Vector A200P/L), relative humidity and temperature gradient (Vaisala PT-100) between two points (2 m and 8 m height). The meteorological measurements were sampled every minute and the 15 min averages were recorded. Precipitation was measured at a 1.5 m height by two tipping buckets (Vaisala and Casella) working in parallel. Radiation measurements were placed at a 3 m height and included incoming and outgoing PAR by Kipp & Zonen PAR-lite sensors, direct and reflected global radiation by Kipp & Zonen CMP-3 pyranometers and net radiation by Kipp & Zonen NR-lite2 net radiometer.

Soil moisture and temperature were measured in one soil profile, having sensors at depths of 5, 20 and 50 cm. There was also a separate soil moisture sensor approximately 10 m away from the soil profile. Soil temperatures were measured with PT100 platinum thermometers, soil moisture with Delta-T sensors, and soil surface energy flux with Hukseflux HFP01 heat flux plate at a 5 cm depth.

Carbon dioxide, water vapour, sensible heat and momentum fluxes were measured using an eddy covariance setup similar to the one described by Aurela et al. (2009). The sonic anemometer was a METEK USA-1, and the CO_2 concentrations were measured using a Li-Cor LI-7000 closedpath gas analyzer. The sampling frequency of these instruments was 10 Hz. The anemometer and the gas sampling tube were installed at a 9 m height, which was well above the average tree height of 2.5 m. The separation distance between the gas sampling tube and the centrer of the anemomer was 20 cm. The flow rate of the sampling system was 6 L min^{-1}. The length of the inlet tube for the LI-7000 gas analyzer was about 20 m. The material of the inlet tube (ID 4 mm, OD 6 mm) was PTFE, and the pump was Dürr A-062 E1. The gas analyzer was calibrated every month with a high-accuracy CO_2 span gas (378 ppm verified by the Cape Point GAW station), and Afrox instrument grade synthetic air with $CO_2 < 0.5$ ppm was continuously used as a reference gas.

The state of the measurement system was continuously monitored by visiting the measurement site once or twice a week. During each visit, the state of the measurements was logged and corrective actions taken as required. During the data analysis the log file was used to check erroneous measurement periods.

2.3 Processing of eddy covariance data

The turbulent fluxes were calculated as 30 min block averages from the 10 Hz raw data after a double rotation of the wind coordinates (McMillen, 1988) and calculation of the CO_2 mixing ratios with respect to dry air by accounting for water vapour fluctuations (Webb et al., 1980). For each averaging period, the time lag between the anemometer and gas analyzer signals was determined using a maximum covariance method. The fluxes were corrected for systematic losses using the transfer function method of Moore (1986). This included a compensation for the low-frequency losses due to block averaging. For the more significant high-frequency losses, an empirical first-order transfer function representing the overall system performance was determined from the field data using the sensible heat flux as a reference. A spectral half-power frequency of 1.6 Hz was determined for CO_2. Generic cospectral distributions (Kaimal and Finnigan, 1994) were assumed for estimating the flux underestimation in different conditions, providing correction factors as a function of wind speed and atmospheric stability. The correction for CO_2 flux loss was 5 % on average.

The storage flux was calculated by assuming a uniform distribution of CO_2 between the soil surface and the measurement height. During the last measurement year, the CO_2 concentration was also measured at a 1.5 m height, which enabled us to calculate a two-point estimate of the storage flux for comparison.

The corrected fluxes of CO_2 were filtered by discarding the data with a friction velocity lower than 0.2 m s^{-1} (18 % of data excluded). Below this limit, the CO_2 flux was observed to increase with increasing friction velocity. In addition, CO_2 fluxes were filtered by setting an acceptable range for average CO_2 concentration (300–500 ppm), gas analyzer sample cell pressure (50–120 kPa) and CO_2 concentration variance (0–10 ppm^2), which resulted in a 3 % loss of flux data in total.

There was only one longer period of malfunction of the gas analyzer, which lasted for 15 days in November 2010. In total, 33 % of the CO_2 flux values in the final time series were missing or discarded, which is similar to the 19-site average of 35 % reported by Falge et al. (2001).

The flux "footprint" area was estimated using the analytical model introduced by Kljun et al. (2004). According to this model, 90 % of the flux originated within a distance of 324 m upwind from the measurement tower. Figure S1 shows the distance of the mean 80 % cumulative flux footprint as a function of wind direction. This footprint area is predominantly located within homogeneous thornveld (Fig. S1).

2.4 Partitioning and gap filling of the CO_2 flux data

The measured net CO_2 flux was partitioned into GPP and ecosystem respiration, R_{eco}, by fitting a respiration function to the night-time data and calculating GPP as the difference between NEE and R_{eco}. Night-time and daytime periods were separated by a threshold PAR value of 20 μmol m^{-2} s^{-1}. The fit parameters were calculated in a moving data window which was defined for each day with an initial length of 6 days. As the data set did not have gaps longer than 15 days, the moving window was expanded up to 20 days if necessary, to cover at least 50 measurement points.

The night-time respiration was calculated using the exponential temperature function:

$$R_{eco} = R_b exp\left(E_0\left(\frac{1}{T_0} - \frac{1}{T_{soil} - T_1}\right)\right) \quad (1)$$

where R_b is the base respiration, E_0 is the temperature sensitivity, T_0 = 56.02 K, T_{soil} is the soil temperature at 5 cm depth and T_1 = 227.13 K (Lloyd and Taylor, 1994). This function was fitted in two steps by first determining the E_0 parameter individually for each year and then fitting the R_b parameter for each data window separately (Lasslop et al., 2010).

The GPP values derived from the NEE observations and R_{eco} estimates were used to fit the hyperbolic tangent function of PAR for every day using data from the 6 to 20 days moving window:

$$\mathrm{GPP}=\mathrm{F}_{\mathrm{p,max}} \cdot \tanh\left(\frac{d \cdot \mathrm{PAR}}{F_{\mathrm{p,max}}}\right) \quad (2)$$

where $F_{p,max}$ is the canopy assimilation at light saturation and d is the initial slope of light response (von Stamm, 1994). The model parameters were determined using the "lsqnonlin" command of MATLAB Release 2015b, which uses a trusted region least squares algorithm. The missing values in the GPP time series were filled with the GPP values calculated using Eq. (2). Finally, the NEE time series was gap filled using the sum of R_{eco} and GPP.

The eddy covariance measurement data used in this study covered the period from September 2010 to August 2013. We analysed the data as one-year periods from 1 September to 31 August, as a growing season at this southern hemispheric site spreads to two consecutive years.

2.5 Uncertainty estimation

The uncertainty in the annual CO_2 budget was estimated by considering the most significant, albeit admittedly not all possible error sources, for both random and systematic errors. For the former, we included the stochastic measurement error inherent in eddy covariance measurements and the error resulting from the gap filling of the CO_2 flux time series for missing data. The random error related to both the stochastic variability and the gap-filling procedure was calculated as a root mean square error by comparing half-hourly values of measured (NEE_{obs}) and modelled (NEE_{mod}) CO_2 fluxes

$$E_{RMS} = \sqrt{\sum \frac{(NEE_{obs} - NEE_{mod})^2}{n}} \quad (3)$$

Where NEE_{mod} was calculated with Eqs. (1) and (2). This procedure assumes that the agreement is not affected by systematic measurement or model errors. It provides a conservative error estimate for the random measurement error (Aurela et al., 2002), and for the gap-filling error also includes the effect of this random variability on the model fit. The annual measurement error, E_{meas}, and gap-filling error, E_{gaps}, were calculated by multiplying E_{RMS} by the square root of the number of accepted measurements and missing data, respectively.

In addition to the random error, the annual systematic error due to friction velocity filtering, E_{ustar}, was estimated based on a sensitivity test in which the full calculation procedure for the annual balance was repeated with modified data sets; these data sets resulted from screening with two additional values of friction velocity (0.15 and 0.25 m s^{-1}) (Aurela et al., 2002). E_{ustar} was estimated as an average deviation from the annual carbon balance calculated using the optimal friction velocity limit (0.20 m s^{-1}).

We estimated the systematic error due to the correction for flux losses described in Sect. 2.3, E_{loss}, and assumed that other systematic errors have been sufficiently compensated for in the post-processing of the eddy covariance data. We calculated the annual error from the mean daytime and night-time fluxes that were determined separately for dry and wet seasons. The uncertainty estimate for our correction coefficients was adopted from Mamadou et al. (2016), who observed that the cospectral functions determined for their grassland site differed from the commonly used generic cospectra (Kaimal and Finnigan, 1994), also used in the present study, which difference has an influence on the correction factors. By using the mean differences in the correction factors (daytime 4 %, night-time 14 %) reported by Mamadou et al. (2016), we could modify the degree of our flux loss correction and estimate the resulting uncertainty in the annual CO_2 balance.

The total uncertainty of the annual carbon balance was calculated by adding the different annual errors in quadrature:

$$E_{tot} = \sqrt{E_{meas}^2 + E_{gaps}^2 + E_{ustar}^2 + E_{loss}^2} \quad (4)$$

2.6 Satellite data

In order to study long-term productivity, monthly averages of NDVI were calculated from the MODIS NBAR (nadir BRDF adjusted reflectance) product MCD43A4 (one 500 m pixel) at the flux footprint of the eddy covariance measurement (Figure S1). This product uses the reflectance data which is adjusted using a bidirectional reflectance distribution function for view angle effects. The NDVI signal is a simple transformation of spectral bands without any bias from ground-based parameters (Huete et al., 2002).

3 Results and discussion

3.1 CO_2 exchange dynamics

Figure 2 shows a time series of incoming PAR, air temperature, precipitation and CO_2 flux for the full measurement period. The incoming PAR and air temperature were highest in January and lowest in July. Precipitation was highest during the growing season 2010–2011 with a yearly sum of 721 mm. The highest inter-annual variation in CO_2 flux occurred during the wet season, whereas during the dry season CO_2 fluxes were rather similar in magnitude.

The daytime canopy carbon assimilation in the middle of the wet season (DJF) followed the common pattern where the daytime CO_2 uptake increased with increasing incoming PAR until it reached a saturated value (Fig. 3). The dry season (JJA) CO_2 flux rates were an order of magnitude lower than the wet season rates and canopy assimilation was rarely

saturated with respect to PAR. On average, the mean daytime NEE decreased with increasing VPD when VPD exceeded a limit of 1 kPa (Fig. S2).

The night-time respiration did not show a clear exponential relationship with either soil moisture or soil temperature in any of the respiration fitting windows, which ranged from 6 to 20 days (data not shown). The highest ranges of soil moisture in individual fitting data sets were from 1 to 7 % during the dry season and from 8 to 21 % during the wet season, but there was no significant relationship with respiration. A clear linear increase in respiration with increasing soil moisture was only observed once, after the first intense rainfall event in early November 2010. Similarly, the night-time respiration did not increase strongly with soil temperature in any of the respiration fitting windows. Instead, the respiration rate remained rather constant with a ~2 μmol m^{-2} s^{-1} reduction at the highest temperatures during the middle part of the wet season in 2010–2011. However, on an annual time scale, higher respiration rates were observed when soil temperatures were higher (Fig. 4). There is little correlation with soil water content during either dry or wet season, or on an annual time scale. Therefore, it seems that the ecosystem respiration is driven by plant phenology, being higher during the rainy seasons and on average unaffected by short-term variations in soil water content and soil temperature. Our respiration relations are similar to those reported by Tagesson et al. (2015), who observed no relationship between the night-time NEE and the environmental drivers for 7-day periods in grazed savanna in Senegal.

Even though the temperature dependency was weak, the respiration rates modelled with Eq. (1) correlated well with the measured respiration (R^2=0.56, $p < 0.01$).

3.2 Diurnal CO_2 cycle

The mean monthly diurnal variation of NEE reveals a change in the ecosystem dynamics during the transition from the dry to wet season (Figs. 5 and 6). The highest values of carbon uptake occurred every year in December or January from 10 am to 12 am (the darkest pixels in Fig. 5), whereas the incoming PAR had its peak between 11 am and 1 pm (data not shown). This phase difference is most likely caused by the stomata closure before the radiation peak, as plants avoid water loss.

To understand the controlling drivers of the diurnal NEE cycle, we analysed the mean monthly diurnal cycle of GPP, respiration and VPD. The diurnal cycles of GPP and respiration show that the monthly diurnal variation of GPP between the years is larger than the variation in respiration (Fig. 6). The mean monthly diurnal cycle of the VPD values above a 1 kPa threshold, VPD_1, shows marked differences from September to November between different years (Fig. 7).

In September the mean diurnal NEE cycle can be depicted by a smooth curve, with a nearly levelled maximal uptake period from 10 am to 3 pm. The diurnal cycle of NEE is positive in September 2012 due to higher respiration rates. In October 2010, the daily peak GPP is about 2 μmol m^{-2} lower than during the other years, which could be due to VPD as VPD_1 was 1 kPa higher than during the other years. In November 2010, the diurnal pattern of NEE showed a sharp dip after the maximal uptake was reached. The peak NEE value in November 2012 was reached already at 9 am, whereas in the other years the November peak NEE value was reached at 11 am. This is explained by the different diurnal cycles of GPP during the other

years (Fig. 6c). From December to February, the differences in the diurnal cycle of NEE are explained by the differences in the GPP cycle. From March to August, the differences in VPD_1 were not large and the largest variation between the years are seen in the diurnal cycle of GPP.

3.3 Intra-annual variation in CO_2 fluxes

In this section, we analyse the differences in carbon fluxes and their environmental drivers at a monthly scale during the three measurement years. This analysis was based on monthly data in order to facilitate comparison between the years, which would not be possible with daily data due to the large scatter in carbon fluxes and environmental variables.

The highest carbon uptake was observed during the growing season 2010–2011 (Figs. 8 and S3). Heavy rainfall occurred from November to January, and soil temperature was relatively low. This contributed to the strong growth of vegetation and large net carbon uptake. Furthermore, VPD was low from January to April, which resulted in continued uptake of carbon. Due to the relatively low soil temperatures throughout the growing season, the yearly respiration in 2010–2011 was lower than during the year 2012–2013.

During the year 2011–2012 the annual rainfall was lower than during the other years; especially the December–January precipitation was low. Moreover, VPD was relatively high during this period and thus the growth of vegetation was weak. In February and March, the carbon balance was positive possibly due to enhanced heterotrophic respiration and a relatively small LAI.

During the year 2012–2013, the total respiration was relatively high already in September. The early rainfall may have led to an early growth of soil microbial populations that enhance the soil respiration capacity during the whole season. Furthermore, respiration was high throughout the growing season due to the consistently higher air and soil temperatures. From December to February, the monthly GPP was relatively high but the net carbon uptake was less than during the year 2010–2011 due to the much higher respiration rates. From February to April, soil moisture was relatively low and VPD was high, and thus the carbon uptake by photosynthesis was limited. This led to the most positive carbon balance of all years. On the other hand, the monthly values of NEE and any of the environmental variables were not linearly correlated ($R^2 < 0.05$, $p > 0.1$). The lack of significant correlations may indicate that also at monthly scale the relation between NEE and the environmental drivers are non-linear and thus it would not be straightforward to separate the effects of the different drivers. Furthermore, confounding effects by phenological variations are likely during the transitions from wet to dry season.

There was roughly a ten-fold difference in the monthly GPP sums between the wet and dry seasons. During the dry season, the grasses are dormant and only trees are contributing to GPP. During the dry season, this contribution did not vary between the years, even though soil moisture varied significantly. Therefore, the inter-annual variation in GPP was largely due to the variation during the wet season.

At a monthly time scale there were two periods which largely determined the inter-annual variation of NEE. Firstly, at the beginning of the rainy season (September to November) NEE showed a large variation which was due to variation in both the respiration and GPP components. Secondly, from December to January the ecosystem was taking up carbon during each

year. During this period the monthly respiration and GPP were highest and the monthly respiration followed precipitation patterns. The primary carbon uptake period spanned from December to January, whereas the total carbon uptake period varied in magnitude and in length from 3 to 6 months. There was some variation in the date of the transition to carbon uptake period, which took place on 20 November in the year 2010–2011 and on 25 November in 2011–2012 whereas in year 2012–2013 this transition took place on 10 December (Fig. S3).

In conclusion, the high precipitation in December and January led to large carbon uptake rates during the growing season. On the other hand, early rainfall in September and the relatively high air and soil temperatures throughout the year resulted in a significantly higher yearly respiration sum and thus in a more positive carbon balance.

3.4 Annual carbon balances

The carbon balances (± uncertainty) from 1 September to 31 August for the years 2010–2011, 2011–2012 and 2012–2013 were -85 ± 16, 67 ± 20 and 139 ± 13 g C m^{-2} yr^{-1}, respectively (Table 3). The total uncertainty for these years was 19 %, 30 % and 9 % of the corresponding annual balance. The mean annual random measurement error was 6 %, the gap-filling error was 4 %, and the friction velocity filtering error was 18 %. The uncertainty due to the systematic flux loss correction error was about 1 % of the annual carbon balances.

While the uncertainty derived for the eddy covariance measurements can be considered moderate, it should be noted that the estimates of the ecosystem carbon balance are also affected by the calculation of storage fluxes. The 2012–2013 CO_2 balance calculated using the two-point estimate for the storage flux was 88 g C m^{-2} yr^{-1}, which was 51 g C m^{-2} yr^{-1} less than the balance based on a single CO_2 concentration measurement level. The one-point storage flux was used for the whole measurement period because the two-point concentration data covered only the last year of measurements. Assuming a similar influence on the annual balance of the other years, the CO_2 balance of the growing season 2011-–2012 remains slightly positive, while that of 2010–2011 becomes even more negative.

The changes in the yearly NEE sum cannot be explained by the changes in annual precipitation, temperature, length of rainy season or peak NDVI. However, the number of days when soil moisture was higher than 7 % is related to the annual NEE sum. The soil moisture of 7 % is thought to be a critical limit below which plants become water stressed (Archibald et al., 2009). Given that our data only covered three years, it is not possible to generalize the relation between the annual carbon balance and the number of wet soil days. Moreover, at monthly and weekly scales the carbon balance and wet soil days were not correlated (Table 3).

The annual GPP variation followed the variation in precipitation and peak NDVI, whereas the relation between the annual respiration and environmental drivers was not clear. As shown in Sect. 3.3, the environmental drivers such as soil moisture and soil temperature do partly control the wet season carbon fluxes, while the carbon balance of a dry season is less sensitive to the changes in these variables. Therefore, the environmental drivers can have a different kind of effect on carbon balance during different seasons. Furthermore, as the annual sum of NEE is a small difference of two large components, i.e. carbon

uptake by photosynthesis and carbon release to the atmosphere by respiration, the NEE sum is sensitive to small changes in its components.

3.5 NDVI as proxy for GPP

There was a strong positive correlation between the monthly sum of GPP and the monthly mean NDVI (R^2=0.83, p<0.001) (Fig. 9). Sjöström et al. (2009) also found a high correlation between the 8-day NDVI mean and GPP sum in Sudanian savanna with a tree cover of 7 %.

Figure 10 shows a 12-year time series of monthly NDVI and precipitation data for Welgegund. The peak value and the shape of the annual cycle of both variables vary significantly between the years. The peak NDVI occurred each year between December and March and it lagged the peak rainfall by 1 or 2 months with the exception of the year 2007. Within our three year flux data period, the peak NDVI was related to the peak GPP in year 2010–2011 and in year 2011–2012 but it did not capture the rainy season peak in GPP in 2012–2013. Based on the NDVI data, it can be concluded that the year 2010–2011 represents a common pattern at this site, whereas in 2011–2012 and 2012–2013 the NDVI peak values were lower than the long-term average.

Scanlon et al. (2002) demonstrated with a 16-year NDVI time series from the Advanced Very High Resolution Radiometer across a rainfall gradient that grassy areas contributed most to the inter-annual variation in NDVI. In addition, trees have been shown to have more consistent phenological cycles in savannas (Archibald and Scholes, 2007). Therefore, according to NDVI dynamics, the Welgegund site shows characteristics of a grassland.

From September 2001 to August 2013, the yearly maximum values of the measurement site NDVI were on average 0.02 units smaller than those of a nearby moist sandy grassland area which is not grazed (land-use class 6 in Fig. S1). This difference is most probably due to heavy grazing at the measurement site.

3.6 Comparison to other sites

The annual NEE sum and its inter-annual variation at our site differ significantly from the results reported by a previous study at a grazed savanna grassland in Dahra, Senegal (Tagesson et al., 2015, 2016b). The Dahra site had a peak MODIS LAI (MOD15A2) between 1.4 to 2.1 and a mean annual precipitation of 524 mm, which are similar to the Welgegund site. However, the yearly carbon balance at Dahra, which varied from -336 to -227 g C m^{-2} during three years, showed that this site is a strong sink. The major difference between these two sites is that the dominant grass species change yearly at Dahra, whereas Welgegund has a perennial grass layer. The large difference in the carbon balance is due to the much larger carbon uptake at Dahra during the rainy seasons, which may be explained by the moderately dense C_4 ground vegetation and high soil nutrient availability.

On the other hand, the carbon balance at our site is similar to the balance measured at the Skukuza site in Kruger National Park, South Africa, which has yearly precipitation similar to Welgegund but a significantly higher tree cover of 30 %

(Archibald et al., 2009). The reason for this agreement in carbon balance is probably the large mammalian herbivore population and fires at the Skukuza site, which make the carbon balance more positive.

At the savanna sites of Nalohou, Benin and Bontioli, Burkina Faso, which have significantly higher annual precipitation (852 and 1190 mm, respectively) and LAI, the carbon balance varied from -429 to -136 g C m^{-2} yr^{-1} (Ago et al., 2014; Brümmer et al., 2008). These sites were not grazed but the grasses were burned annually. During the dry season at the Nalohou site, higher soil moisture resulted in higher soil respiration rates and thus a more positive total carbon balance. In contrast, at the Bontioli site higher precipitation during the transition period from wet to dry season resulted in a higher uptake of carbon. However, at Welgegund the dry season fluxes were an order of magnitude smaller than the wet season fluxes and the dry season carbon balance did not significantly vary between the years. Similarly, the dry season carbon balance did not show significant differences at grassland, cropland and nature reserve sites in the Sudanian Savanna which receives a similar amount of precipitation to the Welgegund site (Quansah et al., 2015).

4 Conclusion

The results of this study indicate that the inter-annual variation of NEE is high at the Welgegund savanna grassland site, as compared with a grazed savanna grassland in Senegal. The carbon balances for the years 2010–2011, 2011–2012 and 2012–2013 were -85 ± 16, 67 ± 20 and 139 ± 13 g C m^{-2} yr^{-1}, respectively. This is similar to the variation at the Kruger National Park where the annual NEE ranged from -138 to 155 g C m^{-2} yr^{-1} during a 5-year measurement period (Archibald et al., 2009).

The night-time respiration was not significantly dependent on either soil moisture or soil temperature on a weekly temporal scale, whereas on an annual time scale higher respiration rates were observed when soil temperatures were higher. Similar results were observed at a West African dry savanna, where none of the environmental variables could explain the half-hourly night-time respiration measurements (Tagesson et al., 2015).

The beginning of the rainy season (September to November) and the mid-growing season (December to January) largely determined the inter-annual variation of carbon balance. An early rainfall in September 2012 and the higher soil temperature resulted in higher respiration rates and thus a more positive carbon balance. During the mid-growing season both the ecosystem respiration and GPP were highest and the monthly respiration rates followed the precipitation patterns.

Future work should focus on the respiration variations during the daytime. With more direct soil respiration measurements and cattle respiratory flux measurements the overall uncertainty of the total ecosystem respiration estimates could be reduced. In addition, these measurements would provide much needed information about the environmental drivers of respiration specific to savanna ecosystems.

Acknowledgements

This work was supported by Finnish Meteorological institute, The North-West University and University of Helsinki, and the Finnish Academy project *Developing the atmospheric measurement capacity in Southern Africa* and Finnish Centre of Excellence, Grant no. 272041. The authors wish to thank Eduardo Maeda for downloading and processing the MODIS NDVI data, South African Weather Service (SAWS) for the provision of the long-term rainfall and temperature data and the farmers at the ranch.

References

Ago, E. E., Agbossou, E. K., Galle, S., Cohard, J.-M., Heinesch, B. and Aubinet, M.: Long term observations of carbon dioxide exchange over cultivated savanna under a Sudanian climate in Benin (West Africa), Agric. For. Meteorol., 197, 13–25, doi:10.1016/j.agrformet.2014.06.005, 2014.

Ahlström, A.: The dominant role of semi-arid ecosystems in the trend and variability of the land CO_2 sink, J. Geophys. Res. Space Phys., 120(6), 4503–4518, doi:10.1002/2015JA021022, 2015.

Archibald, S. and Scholes, R. J.: Leaf green-up in a semi-arid African savanna-separating tree and grass responses to environmental cues, J. Veg. Sci., 18(4), 583–594, 2007.

Archibald, S. A., Kirton, A., van der Merwe, M. R., Scholes, R. J., Williams, C. A. and Hanan, N.: Drivers of inter-annual variability in Net Ecosystem Exchange in a semi-arid savanna ecosystem, South Africa, Biogeosciences, 6(2), 251–266, doi:10.5194/bg-6-251-2009, 2009.

Aurela, M., Lohila, A., Tuovinen, J.-P., Hatakka, J., Riutta, T. and Laurila, T.: Carbon dioxide exchange on a northern boreal fen, Boreal Env. Res, 14(4), 699–710, 2009.

Aurela, M., Laurila, T. and Tuovinen, J.-P.: Annual CO_2 balance of a subarctic fen in northern Europe: Importance of the wintertime efflux, J. Geophys. Res. Atmospheres, 107(D21), ACH 17-1-ACH 17-12, doi:10.1029/2002JD002055, 2002.

Booyens, W., Van Zyl, P. G., Beukes, J. P., Ruiz-Jimenez, J., Kopperi, M., Riekkola, M.-L., Josipovic, M., Venter, A. D., Jaars, K., Laakso, L., Vakkari, V., Kulmala, M. and Pienaar, J. J.: Size-resolved characterisation of organic compounds in atmospheric aerosols collected at Welgegund, South Africa, J. Atmospheric Chem., 72(1), 43–64, doi:10.1007/s10874-015-9304-6, 2015.

Brümmer, C., Falk, U., Papen, H., Szarzynski, J., Wassmann, R. and Brüggemann, N.: Diurnal, seasonal, and interannual variation in carbon dioxide and energy exchange in shrub savanna in Burkina Faso (West Africa), J. Geophys. Res. Biogeosciences, 113(2), doi:10.1029/2007JG000583, 2008.

Falge, E., Baldocchi, D., Olson, R., Anthoni, P., Aubinet, M., Bernhofer, C., Burba, G., Ceulemans, R., Clement, R., Dolman, H., Granier, A., Gross, P., Grünwald, T., Hollinger, D., Jensen, N.-O., Katul, G., Keronen, P., Kowalski, A., Lai, C. T., Law, B. E., Meyers, T., Moncrieff, J., Moors, E., Munger, J. W., Pilegaard, K., Rannik, Ü., Rebmann, C., Suyker, A.,

Tenhunen, J., Tu, K., Verma, S., Vesala, T., Wilson, K. and Wofsy, S.: Gap filling strategies for defensible annual sums of net ecosystem exchange, Agric. For. Meteorol., 107(1), 43–69, doi:10.1016/S0168-1923(00)00225-2, 2001.

Grace, J., Jose, J. S., Meir, P., Miranda, H. S. and Montes, R. A.: Productivity and carbon fluxes of tropical savannas, J. Biogeogr., 33(3), 387–400, doi:10.1111/j.1365-2699.2005.01448.x, 2006.

Huete, A., Didan, K., Miura, T., Rodriguez, E. P., Gao, X. and Ferreira, L. G.: Overview of the radiometric and biophysical performance of the MODIS vegetation indices, Remote Sens. Environ., 83(1), 195–213, 2002.

Kaimal, J. C. and Finnigan, J. J.: Atmospheric Boundary Layer Flows. Their Structure and Measurement, Oxford University Press, New York, 304 pp., 1994.

Jaars, K., Beukes, J. P., van Zyl, P. G., Venter, A. D., Josipovic, M., Pienaar, J. J., Vakkari, V., Aaltonen, H., Laakso, H., Kulmala, M., Tiitta, P., Guenther, A., Hellén, H., Laakso, L. and Hakola, H.: Ambient aromatic hydrocarbon measurements at Welgegund, South Africa, Atmospheric Chem. Phys., 14(13), 7075–7089, doi:10.5194/acp-14-7075-2014, 2014.

Kljun, N., Calanca, P., Rotach, M. W. and Schmid, H. P.: A Simple Parameterisation for Flux Footprint Predictions, Bound.-Layer Meteorol., 112(3), 503–523, doi:10.1023/B:BOUN.0000030653.71031.96, 2004.

Kotze, I. and Rose, M.: Farming facts and futures: Reconnecting South Africa's food systems to its ecosystems, Cape Town South Afr. WWF-SA, 2015.

Kutsch, W. L., Hanan, N., Scholes, B., McHugh, I., Kubheka, W., Eckhardt, H. and Williams, C.: Response of carbon fluxes to water relations in a savanna ecosystem in South Africa, Biogeosciences, 5(6), 1797–1808, doi:10.5194/bg-5-1797-2008, 2008.

Laakso, L., Beukes, J. P., Van Zyl, P. G., Pienaar, J. J., Josipovic, M., Venter, A. Jaars, K., Vakkari, V., Labuschagne, C., Chiloane, K. and Tuovinen, J.-P.: Ozone concentrations and their potential impacts on vegetation in southern Africa. Developments in Environmental Science 13, 429-450, 2013.

Lloyd, J. and Taylor, J. A.: On the temperature dependence of soil respiration, Funct. Ecol., 315–323, 1994.

Lasslop, G., Reichstein, M., Papale, D., Richardson, A. D., Arneth, A., Barr, A., Stoy, P. and Wohlfahrt, G.: Separation of net ecosystem exchange into assimilation and respiration using a light response curve approach: critical issues and global evaluation, Glob. Change Biol., 16(1), 187–208, doi:10.1111/j.1365-2486.2009.02041.x, 2010.

McMillen, R. T.: An eddy correlation technique with extended applicability to non-simple terrain. Boundary-Layer Meteorol., 43, 231–245, 1988.

Merbold, L., Ardö, J., Arneth, A., Scholes, R. J., Nouvellon, Y., de Grandcourt, A., Archibald, S., Bonnefond, J. M., Boulain, N., Brueggemann, N., Bruemmer, C., Cappelaere, B., Ceschia, E., El-Khidir, H. A. M., El-Tahir, B. A., Falk, U., Lloyd, J., Kergoat, L., Le Dantec, V., Mougin, E., Muchinda, M., Mukelabai, M. M., Ramier, D., Roupsard, O., Timouk, F., Veenendaal, E. M. and Kutsch, W. L.: Precipitation as driver of carbon fluxes in 11 African ecosystems, Biogeosciences, 6(6), 1027–1041, doi:10.5194/bg-6-1027-2009, 2009.

Mamadou, O., Gourlez de la Motte, L., De Ligne, A., Heinesch, B. and Aubinet, M.: Sensitivity of the annual net ecosystem exchange to the cospectral model used for high frequency loss corrections at a grazed grassland site, Agric. For. Meteorol., 228–229, 360–369, doi:10.1016/j.agrformet.2016.06.008, 2016.

Moore, C. J.: Frequency response corrections for eddy correlation systems, Boundary-Layer Meteorol., 37, 17–35, 1986.

Quansah, E., Mauder, M., Balogun, A. A., Amekudzi, L. K., Hingerl, L., Bliefernicht, J. and Kunstmann, H.: Carbon dioxide fluxes from contrasting ecosystems in the Sudanian Savanna in West Africa, Carbon Balance Manag., 10(1), doi:10.1186/s13021-014-0011-4, 2015.

Reichstein, M., Rey, A., Freibauer, A., Tenhunen, J., Valentini, R., Banza, J., Casals, P., Cheng, Y., Grünzweig, J. M., Irvine, J., Joffre, R., Law, B. E., Loustau, D., Miglietta, F., Oechel, W., Ourcival, J.-M., Pereira, J. S., Peressotti, A., Ponti, F., Qi, Y., Rambal, S., Rayment, M., Romanya, J., Rossi, F., Tedeschi, V., Tirone, G., Xu, M. and Yakir, D.: Modeling temporal and large-scale spatial variability of soil respiration from soil water availability, temperature and vegetation productivity indices, Glob. Biogeochem. Cycles, 17(4), doi:10.1029/2003GB002035, 2003.

Scanlon, T. M., Albertson, J. D., Caylor, K. K. and Williams, C. A.: Determining land surface fractional cover from NDVI and rainfall time series for a savanna ecosystem, Remote Sens. Environ., 82(2), 376–388, 2002.

Scholes, R. and Walker, H.: An African Savanna: synthesis of the Nylsvley study, Cambridge University Press., 1993.

Sjöström, M., Ardö, J., Eklundh, L., El-Tahir, B. A., El-Khidir, H. A. M., Hellström, M., Pilesjö, P. and Seaquist, J.: Evaluation of satellite based indices for gross primary production estimates in a sparse savanna in the Sudan, Biogeosciences, 6(1), 129–138, 2009.

Tagesson, T., Fensholt, R., Cropley, F., Guiro, I., Horion, S., Ehammer, A. and Ardö, J.: Dynamics in carbon exchange fluxes for a grazed semi-arid savanna ecosystem in West Africa, Agric. Ecosyst. Environ., 205, 15–24, doi:10.1016/j.agee.2015.02.017, 2015.

Tagesson, T., Fensholt, R., Cappelaere, B., Mougin, E., Horion, S., Kergoat, L., Nieto, H., Mbow, C., Ehammer, A., Demarty, J. and Ardö, J.: Spatiotemporal variability in carbon exchange fluxes across the Sahel, Agric. For. Meteorol., 226–227, 108–118, doi:10.1016/j.agrformet.2016.05.013, 2016.

Tagesson, T., Ardö, J., Guiro, I., Cropley, F., Mbow, C., Horion, S., Ehammer, A., Mougin, E., Delon, C., Galy-Lacaux, C. and Fensholt, R.: Very high CO_2 exchange fluxes at the peak of the rainy season in a West African grazed semi-arid savanna ecosystem, Geogr. Tidsskr.-Dan. J. Geogr., 116(2), 93–109, doi:10.1080/00167223.2016.1178072, 2016b.

Vakkari, V., Kerminen, V.-M., Beukes, J. P., Tiitta, P., van Zyl, P. G., Josipovic, M., Venter, A. D., Jaars, K., Worsnop, D. R., Kulmala, M. and Laakso, L.: Rapid changes in biomass burning aerosols by atmospheric oxidation, Geophys. Res. Lett., 41(7), 2644–2651, doi:10.1002/2014GL059396, 2014.

Vakkari, V., Tiitta, P., Jaars, K., Croteau, P., Beukes, J. P., Josipovic, M., Kerminen, V.-M., Kulmala, M., Venter, A. D., van Zyl, P. G., Worsnop, D. R. and Laakso, L.: Reevaluating the contribution of sulfuric acid and the origin of organic compounds in atmospheric nanoparticle growth: Reevaluating Nanoparticle Growth, Geophys. Res. Lett., 42(23), 10,486-10,493, doi:10.1002/2015GL066459, 2015.

Valentini, R., Arneth, A., Bombelli, A., Castaldi, S., Cazzolla Gatti, R., Chevallier, F., Ciais, P., Grieco, E., Hartmann, J., Henry, M., Houghton, R. A., Jung, M., Kutsch, W. L., Malhi, Y., Mayorga, E., Merbold, L., Murray-Tortarolo, G., Papale, D., Peylin, P., Poulter, B., Raymond, P. A., Santini, M., Sitch, S., Vaglio Laurin, G., van der Werf, G. R., Williams, C. A. and Scholes, R. J.: A full greenhouse gases budget of Africa: synthesis, uncertainties, and vulnerabilities, Biogeosciences, 11(2), 381–407, doi:10.5194/bg-11-381-2014, 2014.

Veenendaal, E. M., Kolle, O. and Lloyd, J.: Seasonal variation in energy fluxes and carbon dioxide exchange for a broad-leaved semi-arid savanna (Mopane woodland) in Southern Africa, Glob. Change Biol., 10(3), 318–328, 2004.

von Stamm, S.: Linked stomata and photosynthesis model for Corylus avellana (hazel), Ecol. Model., 75–76, 345–357, doi:10.1016/0304-3800(94)90031-0, 1994.

Webb, E. K., Pearman, G. I. and Leuning, R.: Correction of flux measurements for density effects due to heat and water vapour transfer, Q. J. R. Meteorol. Soc., 106(447), 85–100, 1980.

Tables

Table 1. Dominant plant species within the flux footprint. The plant species name is written in italics whereas the roman text refers to the author. Some author names are abbreviated.

Species	Growth form	Mean leaf area (cm^2)	Mean height (m)	Mean canopy (m)	Number of individuals
Vachellia erioloba (E.Mey.) P.J.H.Hurter	Tree	5.9	3.2	1.8	16
Searsia pyroides (Burch.) Moffett	Tree	8.2	2.9	1.2	9
Celtis africana Burm.f.	Tree	18	3.4	1.4	6
Ehretia rigida (Thunb.) Druce	Tree	4.1	2.5	1.8	5
Vachellia karroo (Hayne) Banfi & Galasso	Tree	9.4	2.4	1.6	3
Diospyros lycioides Desf.	Shrub	7.9	1.8	0.8	7
Asparagus laricinus Burch.	Shrub	0.7	1.5	1.1	6
Asparagus suaveolens Burch.	Shrub	0.5	1.3	0.9	4
Grewia flava DC.	Shrub	6.7	2.2	1.8	3

Pentzia globosa Less.	Forb		< 0.5		18
Walafrida densiflora Rolfe	Forb		< 0.5		11
Hermannia depressa N.E. Br.	Forb		< 0.5		8
Dicoma tomentosa Cass.	Forb		< 0.5		6
Euphorbia inaequilatera Sond.	Forb		< 0.5		4
Panicum maximum Jacq.	Graminoid		< 1.5		18
Setaria sphacelata (Schumach.) Stapf & C.E.Hubb. ex Moss	Graminoid		< 1.5		14
Eragrostis trichophora Coss. & Durieu	Graminoid		< 1.5		11
Themeda triandra Forssk.	Graminoid		< 1.5		10
Eragrostis curvula (Schrad.) Nees	Graminoid		< 1.5		9

480 **Table 2.One-sided leaf area index and leaf biomass within the flux footprint area in 2011-2012.**

Sampling date	**Herbaceous LAI**	**Woody LAI**	**Total LAI [m^2 m^{-2}]**	**Herbaceous LAI/ Total LAI [%]**	**Herbaceous [g m^{-2}]**	**Woody [g m^{-2}]**	**Total [g m^{-2}]**
15.4.2011	1.20	1.12	2.32	51.7	383	261	644
16.7.2011	0.12	0.25	0.37	32.4	147	86	233
16.10.2011	0.30	0.47	0.77	39.0	108	169	277
16.1.2012	0.53	0.79	1.32	40.2	157	224	381

485

Table 3. Annual carbon balance and key environmental drivers calculated for each year from September to the August of the following year.

	NEE [gC m^{-2} yr^{-1}]	GPP [gC m^{-2} yr^{-1}]	Respiration [gC m^{-2} yr^{-1}]	Annual precipitation[mm]	Rainy season length [days]	Peak NDVI	Number of days when soil moisture was higher than 7 %	Annual total PAR [mol m^{-2}]
2010	-85 ± 16	-1360	1275	721	207	0.53	232	15500
2011	67 ± 20	-1014	1080	422	178	0.43	101	15300
2012	139 ± 13	-1179	1318	615	228	0.44	79	15500

490

495

Figures

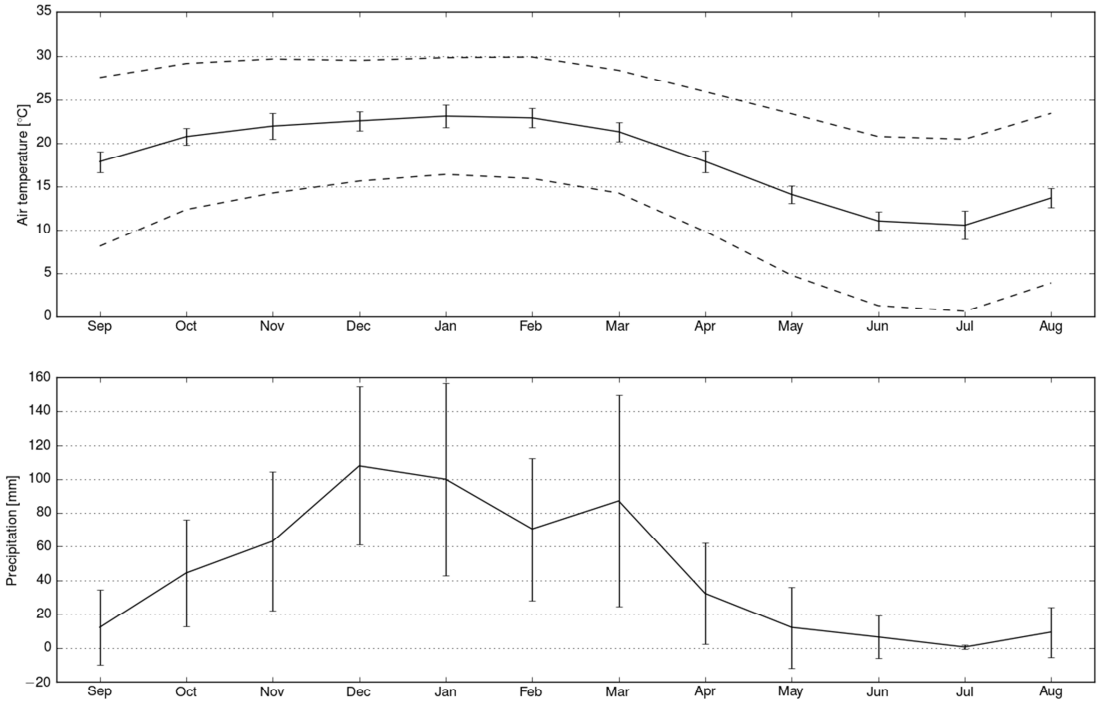

Figure 1. Monthly mean meteorological data from a nearby weather station in Potchefstroom during 1998-2014. The upper figure shows the mean (solid line) and minimum and maximum (dashed lines) air temperatures. The lower figure shows the mean precipitation. Error bars indicate ±1 standard deviation.

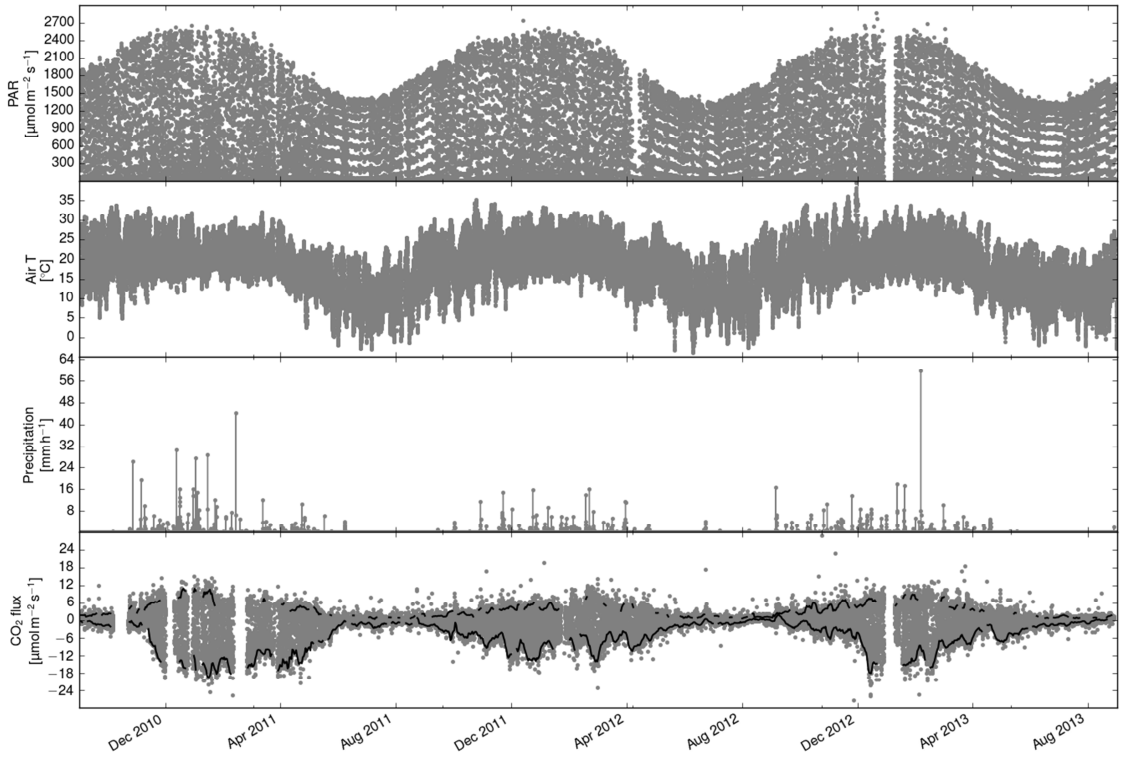

Figure 2. Time series of incoming PAR, air temperature, precipitation and CO_2 flux for the measurement period from September 2010 to August 2013. The solid lines within the CO_2 flux data show the five day centered mean of minimum daytime and maximum night-time CO_2 flux. Incoming PAR, air temperature and CO_2 flux data are 30 minute averages.

510

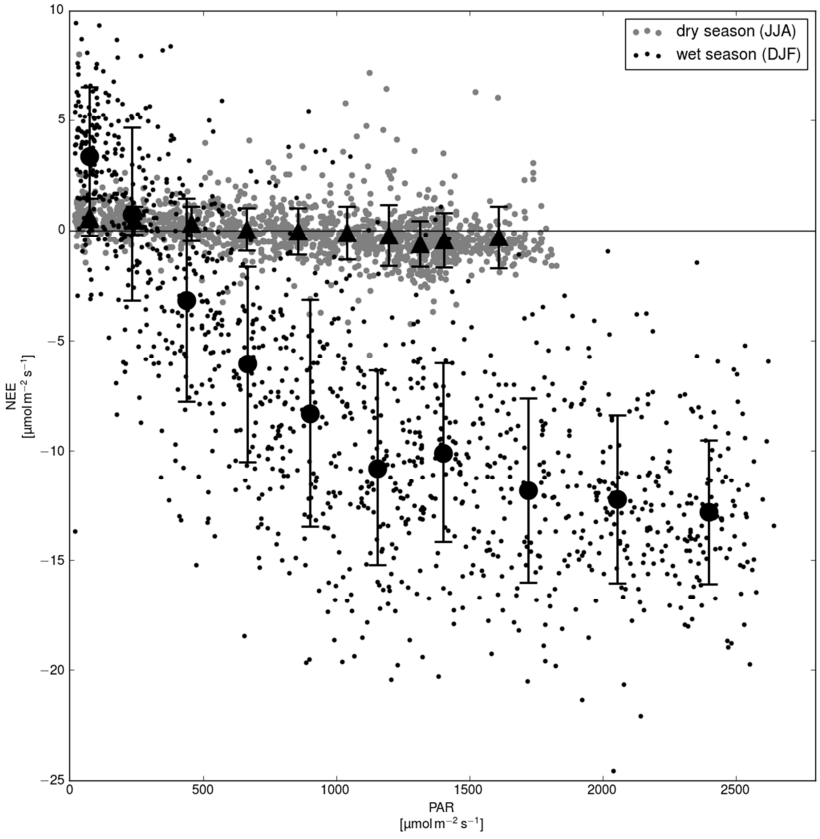

Figure 3. Relationship between PAR and daytime NEE for wet (DJF) and dry (JJA) seasons from September 2010 to August 2011. The triangles (dry season) and circles (wet season) indicate bin averaged values and error bars indicate ±1 standard deviation. Daytime was defined as periods when PAR is higher than 20 μmol m^{-2} s^{-1}. Each bin in dry season contained 157 values whereas the wet season bins contained 125 values.

530

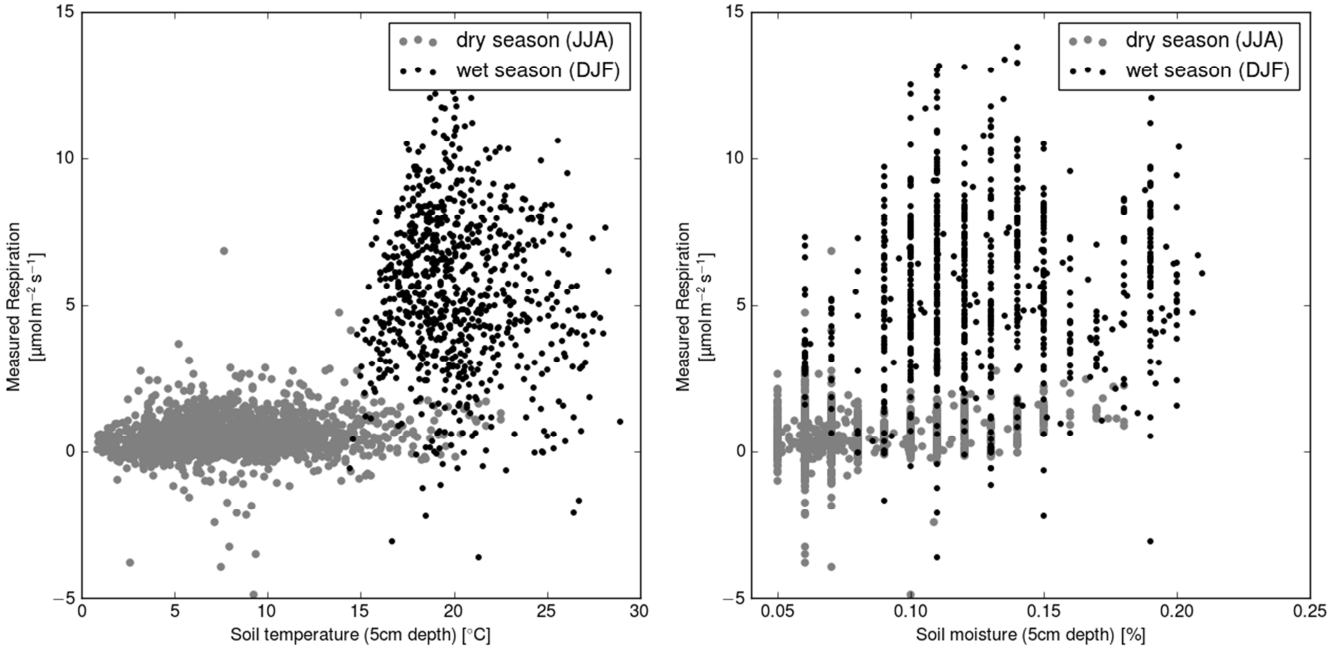

Figure 4. Relationship between night-time respiration and soil temperature (left) and soil moisture (right) for wet (DJF) and dry (JJA) seasons from September 2010 to August 2011. Night-time was defined as periods when PAR is less than 20 µmol m^{-2} s^{-1}.

535

540

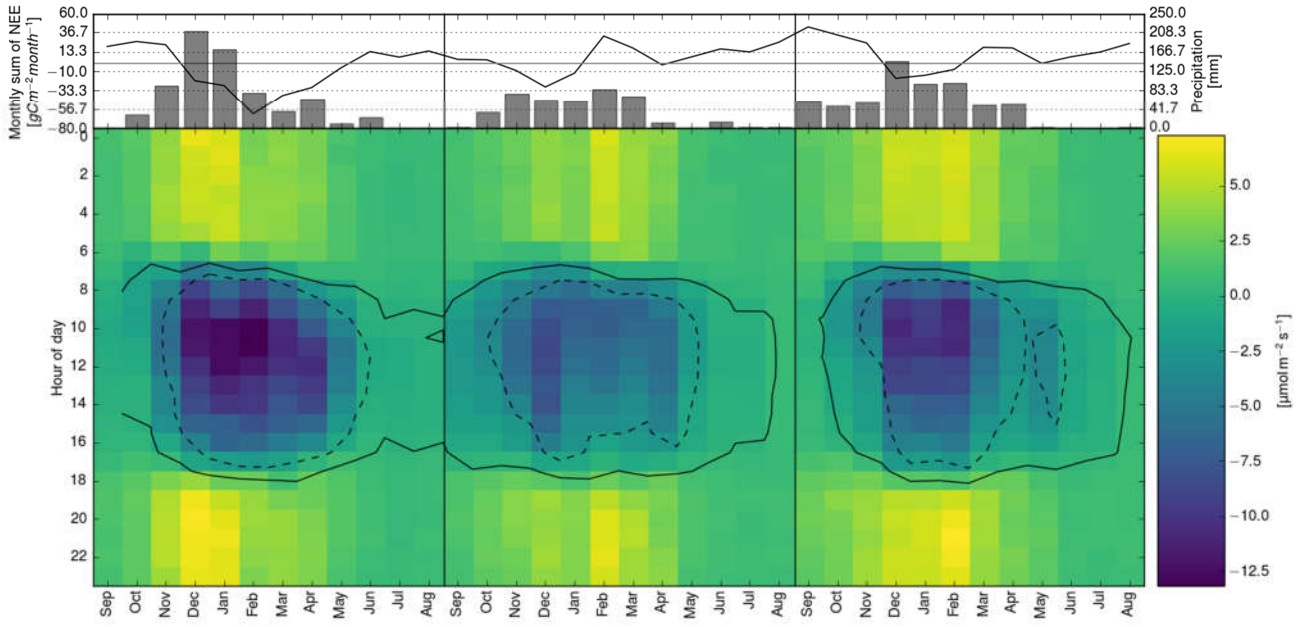

Figure 5. Contour plot of monthly mean NEE for each hour of day. The solid line shows the zero isoline and the dashed line shows the NEE values less than –0.1 µmol m^{-2} s^{-1}. The upper panel shows the monthly NEE as a solid line and the monthly precipitation as bars.

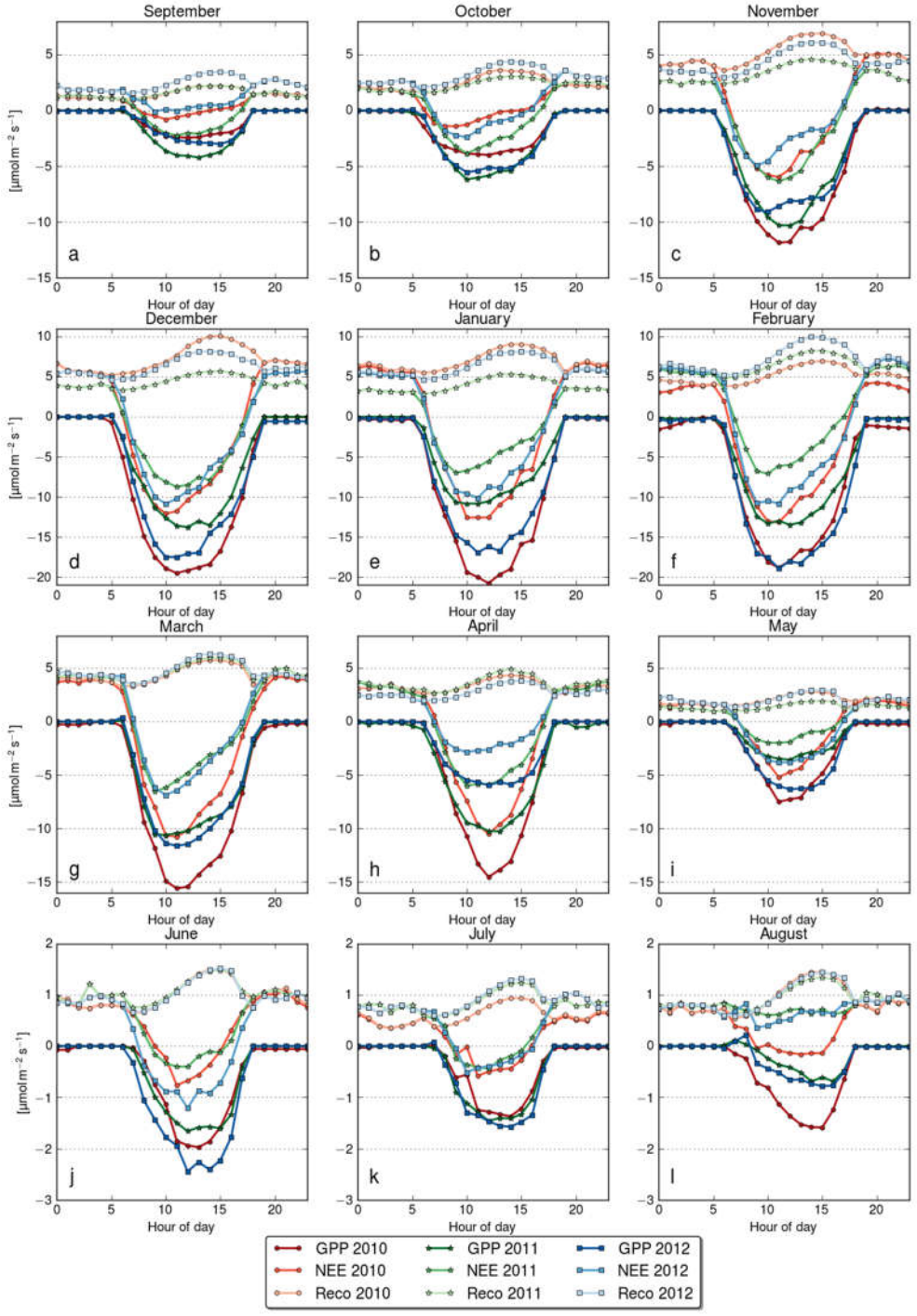

Figure 6. Monthly mean diurnal cycle of GPP, respiration and NEE for each month of the years 2010, 2011 and 2012.

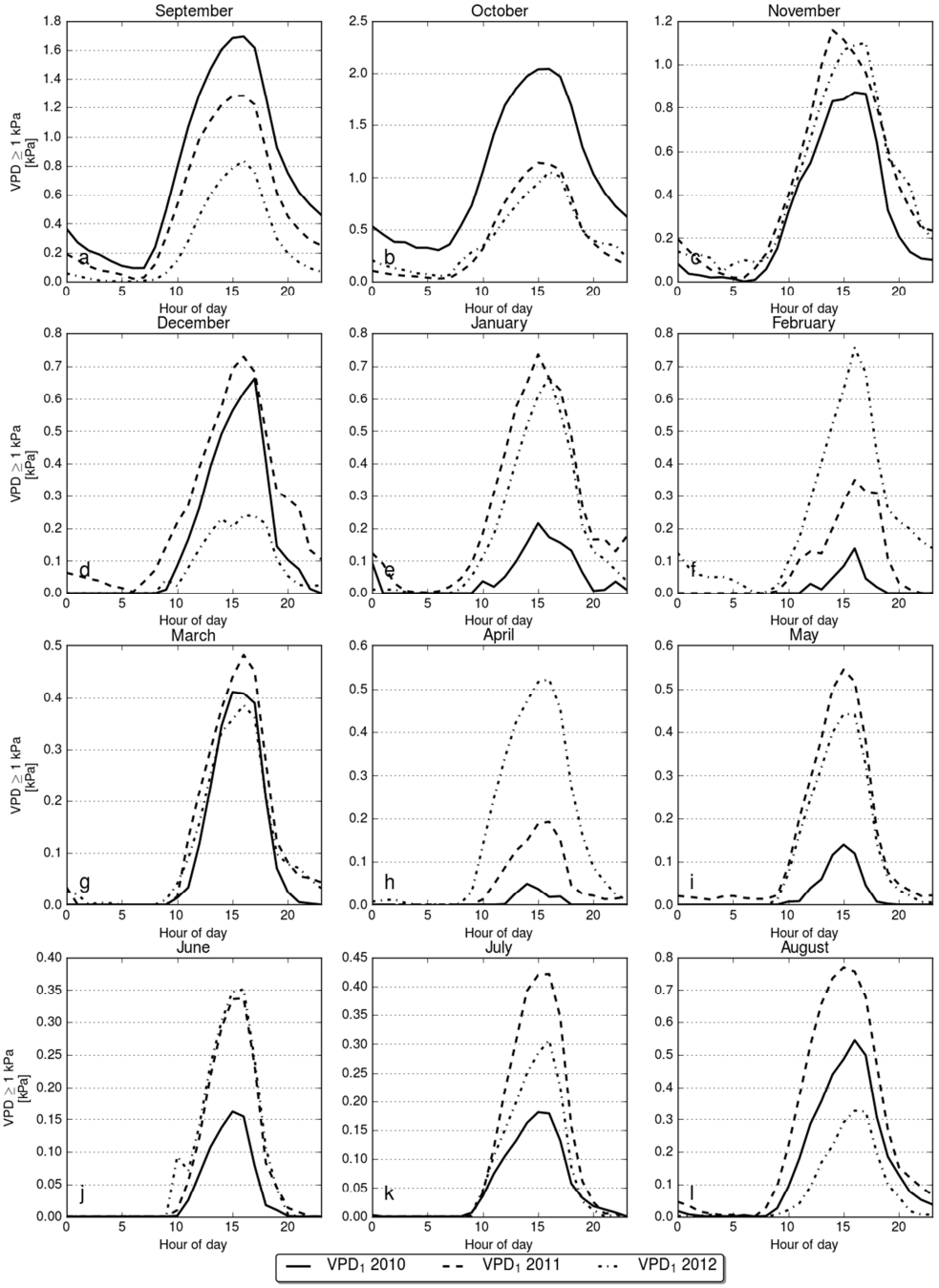

Figure 7. Monthly mean diurnal cycle of the VPD values above 1 kPa, VPD_1, for yearly periods between 1st of September and 31 of August years 2010, 2011 and 2012.

625

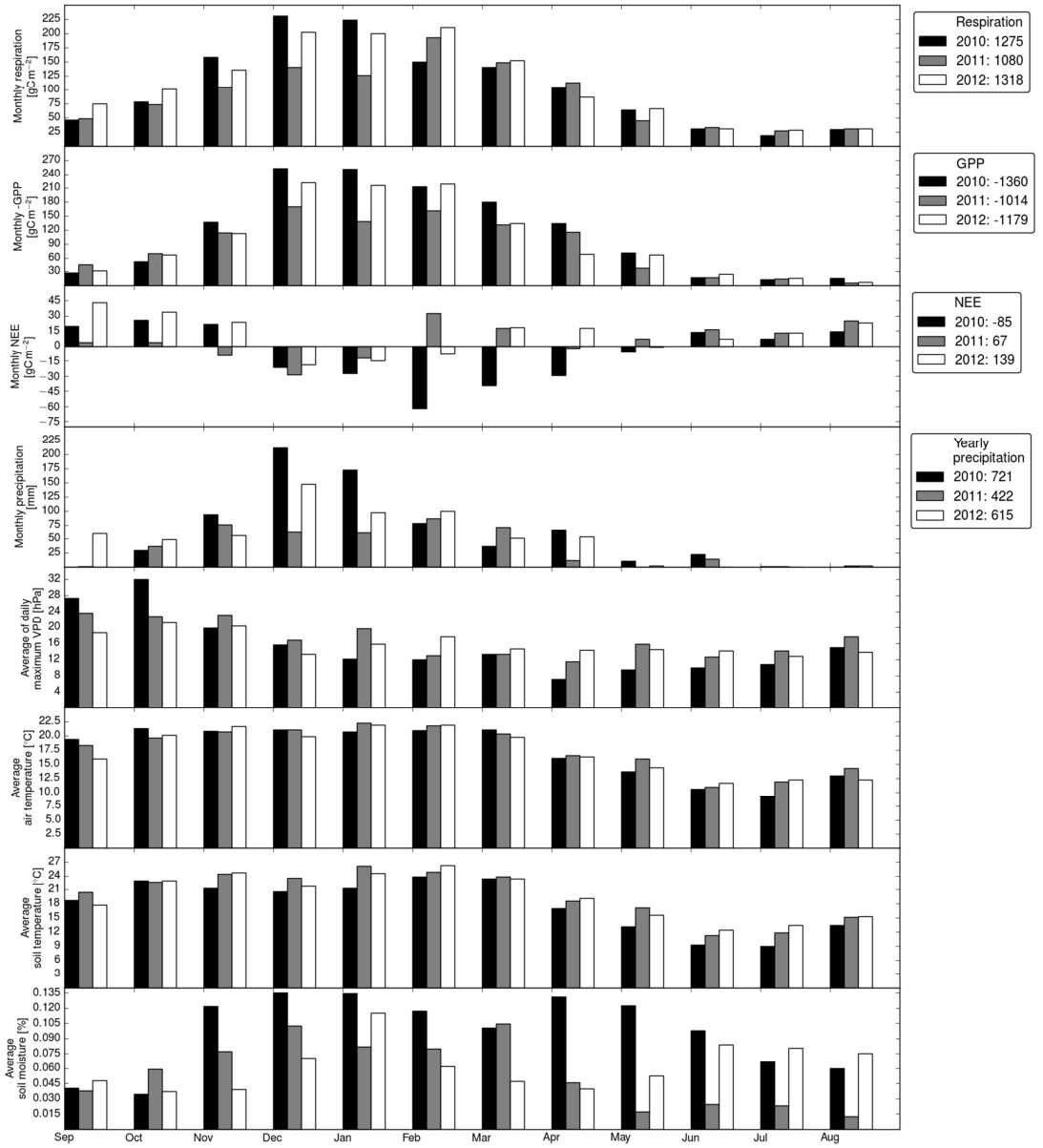

Figure 8. Monthly sums of respiration, GPP, NEE, precipitation and the monthly average of air temperature, soil temperature, soil moisture and daily maximum VPD. The panels on the right side show the yearly sums for the years 2010-2011, 2011-2012 and 2012-2013.

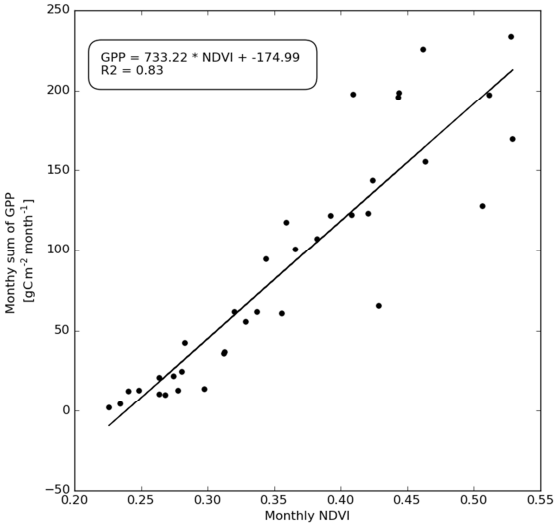

Figure 9. Linear regression between monthly NDVI and monthly sum of GPP.

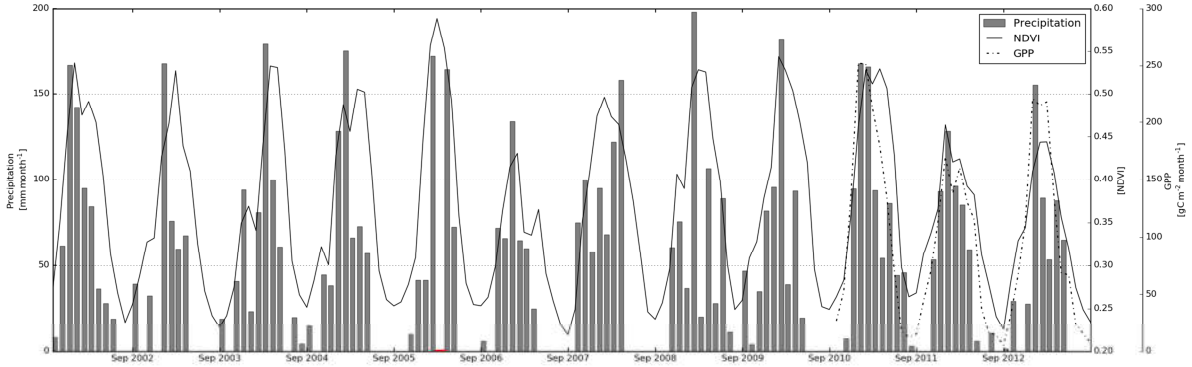

Figure 10. Time series of monthly precipitation (bars), NDVI (solid line) from September 2001 to August 2013 and GPP from September 2010 to August 2013. The precipitation was measured at a nearby weather station (SAWS) in Potchefstroom. The red bar denotes a missing precipitation value in February 2006.

675